

Multi-graph Graph Matching for Coronary Artery Semantic Labeling

Chen Zhao¹, Zihui Xu², Pukar Baral³, Michel Esposito⁴, and Weihua Zhou^{3,5}

¹ Department of Computer Science, Kennesaw State University, Marietta GA, USA

² Department of Cardiology, The First Affiliated Hospital of Nanjing Medical University, Nanjing, China

³ Department of Applied Computing, Michigan Technological University, Houghton, MI, USA

⁴ Department of Cardiology, Medical University of South Carolina, Charleston, SC, USA

⁵ Center for Biocomputing and Digital Health, Institute of Computing and Cyber-systems, and Health Research Institute, Michigan Technological University, Houghton, MI, USA whzhou@mtu.edu

Abstract. Coronary artery disease (CAD) stands as the leading cause of death worldwide, and invasive coronary angiography (ICA) remains the gold standard for assessing vascular anatomical information. However, deep learning-based methods encounter challenges in generating semantic labels for arterial segments, primarily due to the morphological similarity between arterial branches. To address this challenge, we model the vascular tree as a graph and propose a multi-graph graph matching (MGM) algorithm for coronary artery semantic labeling. The MGM algorithm assesses the similarity between arterials in multiple vascular tree graphs, taking into account the cycle consistency between each pair of graphs. This ensures that unannotated arterial segments are appropriately labeled by matching them with annotated segments. Through the incorporation of anatomical graph structure, radiomics features, and semantic mapping, the proposed MGM model achieves an impressive accuracy of 0.9471 for coronary artery semantic labeling. This approach presents a novel tool for coronary artery analysis using ICA videos, offering valuable insights into vascular health and pathology.

Keywords: Coronary artery disease · Invasive coronary angiography · Deep learning · Graph matching

1 Introduction

Coronary artery disease (CAD) is the leading cause of death worldwide and is associated with 17.8 million deaths annually [1]. In the clinical practice of CAD diagnosis, invasive coronary angiography (ICA) continues to serve as the gold standard [2]. This diagnostic technique is crucial for assisting cardiologists in detecting blockages within coronary arteries. With the extracted individual arterial segments, automated identification of these anatomical branches offers

valuable insights for generating reports for CAD. This includes quantifying and evaluating stenosis, as well as quantifying regions of interest, such as fractional flow reserve [19]. However, it is important to recognize the inherent limitations associated with the subjective visual assessment of ICAs [6].

The coronary vascular system comprises two major components: the left coronary artery (LCA) and the right coronary artery trees. The clinical significance of the LCA lies in its role as the primary supplier of blood to the left ventricle [7]. The LCA further branches into three main coronary arteries: the left anterior descending (LAD) artery, the left circumflex (LCX) artery, and the left main artery (LMA). The LAD gives rise to diagonal branches (D), while the LCX gives rise to obtuse marginal (OM) branches. However, semantic labeling of coronary arteries faces challenges when relying solely on position and imaging features [20]. The complexity arises from diverse view angles in ICAs and morphological similarities among different artery branches. These challenges underscore the need for innovative approaches in coronary artery semantic labeling.

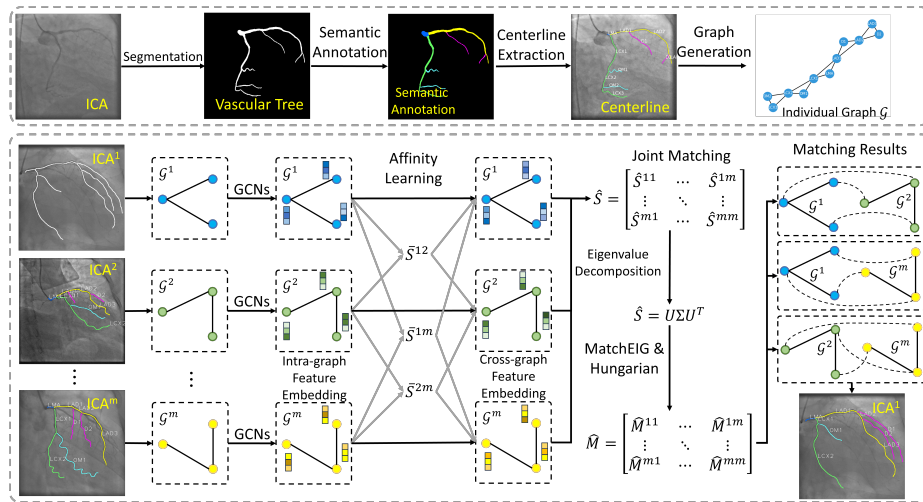


Fig. 1. Workflow of MGM for coronary artery semantic labeling. *top*: individual graph generation; *bottom*: MGM among individual graphs derived from a set of ICAs.

Previously, graph matching has been confined to the comparison of two ICA-generated vascular trees [4,5] for coronary artery semantic labeling. However, graph matching between two ICAs may not capture the complexity inherent in the arterial anatomy. This paper addresses the critical task of coronary artery semantic labeling using multi-graph graph matching (MGM), which incorporates multiple vascular tree structures obtained from various ICA frames, as shown in Fig. 1. The innovation lies in extending graph matching to operate across multiple graphs simultaneously. The arteries in the unlabeled ICA^1 are matched with the arteries in the labeled templates ICA^2 to ICA^m using the node-to-node

Table 1. View angles and number of enrolled subjects

Site	View	Left Anterior Oblique	Right Anterior Oblique	Anterior-Posterior	TOTAL
Site 1	Cranial	42	19	18	79
Site 1	Caudal	18	116	56	190
Site 2	Cranial	44	16	123	183
Site 2	Caudal	20	220	26	266
Total		124	371	223	718

correspondence by MGM. The incorporation of cycle consistency further enhances the accuracy of the matching process, offering a sophisticated solution to the challenges posed by the morphological similarity between arterial branches. Experimental results indicated that the proposed MGM-based coronary artery semantic labeling algorithm achieved an average accuracy of 0.9471. This paper presents a paradigm shift in coronary artery semantic labeling using multi-ICAs joint analysis, opening new avenues for improved understanding and analysis of vascular anatomy and pathology.

2 Materials and Proposed Method

2.1 Enrolled Subjects and Image Pre-processing

Enrolled Subjects In this study, 263 and 455 ICAs from the Medical University of South Carolina and The First Affiliated Hospital of Nanjing Medical University are enrolled, respectively. Each center received local ethical approval from its institutional review board to retrieve and anonymize retrospective, routinely available clinical data. Experienced cardiologists annotated and confirmed the semantic labels of coronary arteries. In each ICA, the LMA, LAD, LCX, OM, and D branches were annotated if present in the subject. All the images were resized into 512×512 . Table 1 shows the number of images in each view angle.

Individual Graph Generation The top of Fig. 1 depicts the workflow to generate the individual arterial graph. The application of FP-U-Net++ [3] is utilized for the extraction of the vascular tree, accompanied by the assignment of pixel-level semantic labels by experienced cardiologists. The arterial centerline is obtained through an edge-linking algorithm [21], and then we separate the centerline into different branches to construct the arterial graph, where *nodes* indicate arterial segments, and *edges* denote connections. 121 features, including the topology, pixel characteristics, and positional attributes, as detailed in [4], are extracted from each node. Formally, each arterial graph is represented by an undirected acyclic graph $\mathcal{G} = (\mathbb{V}, \mathbb{E}, \mathcal{V})$, where $\mathbb{V} = \{\mathbb{V}_1, \dots, \mathbb{V}_n\}$ represents the node set with n nodes; $\mathbb{E} = \{\mathbb{E}_1, \mathbb{E}_2, \dots, \mathbb{E}_{n_e}\}$ represents the edge set with n_e edges, containing the connectivity between arterial branches; $\mathcal{V} = \{v_1, \dots, v_n\}$ indicates features for nodes.

2.2 Multi-graph Graph Matching

The graph matching between two graphs aims to build the node-to-node correspondence between each of the node pairs for each pair of the graphs [8,9], as denoted as the binary permutation matrix $M^{IJ} \in \mathbb{R}^{n_I \times n_J}$, where n_I and n_J represents the number of nodes in I -th and J -th graphs. M_{ij}^{IJ} represents the similarity between the two arterial segments $\mathbb{V}_i^I \in \mathcal{G}^I$ and $\mathbb{V}_j^J \in \mathcal{G}^J$. For MGM, we further consider cycle consistency, which denotes a condition where the matching between *any two* graphs is consistent when passed through any other graphs. Given a set of graph $\mathbb{G} = \{\mathcal{G}^1, \mathcal{G}^2, \dots, \mathcal{G}^m\}$, the cycle consistency is represented by $M^{IJ} = M^{IK} \cdot M^{KJ}$ s.t. $I, J, K \in \{1, \dots, m\}$. Note that we use lowercase i, j, k to represent the index of nodes and uppercase I, J, K to represent the index of graphs. By applying the proposed MGM to the graphs generated by one unlabeled ICA and $m - 1$ labeled ICAs, the artery segments are matched, so that semantic labeling is achieved. The proposed MGM model for coronary artery semantic labeling includes 3 modules.

Intra-graph Feature Embedding and Affinity Learning The feature embedding module aims to capture the essential representation of each arterial segment using Graph Convolutional Networks (GCNs) and multi-layer perceptron (MLP). Given a graph \mathcal{G} , the intra-graph feature embedding for node \mathbb{V}_i in \mathcal{G} is denoted in Eq. 1.

$$v_i^{(l+1)} = \phi_v^{(l)}([\sum_{j \in E_i} v_j^{(l)}, v_i^{(l)}]) \quad (1)$$

where $l \in \{1, \dots, L\}$ represents the index of GCN layers; $\phi_v^{(l)}$ is the MLP for l -th layer; E_i contains the edges connected with node \mathbb{V}_i ; $\sum_{j \in E_i} \cdot$ indicates the element-wise summation of the features from the adjacent nodes; $[\cdot]$ indicates feature concatenation. As a result, Eq. 1 represents the message passing and aggregation for feature embedding using GCN in graph \mathcal{G} .

Given two graphs \mathcal{G}^I and \mathcal{G}^J , the intra-graph node similarity is computed by the weighted dot product of the updated feature embedding for each node pair. Then, a Sinkhorn operator [12] converts the node similarity matrix into a doubly-stochastic matrix as node affinity, as shown in Eq. 2.

$$\bar{S}_{ij}^{IJ} = \mathbf{Sinkhorn}\left(\frac{(v_i^I)^{(L)} \cdot A \cdot (v_j^J)^{(L)}}{\sqrt{d}}\right) \quad (2)$$

where i and j are the node indices; d is the dimension of embedded features; and $A \in \mathbb{R}^{d \times d}$ contains learnable parameters for the node affinity. As a result, the intra-graph node affinity \bar{S} indicates the initial graph matching assignment between each node pair from \mathcal{G}^I and \mathcal{G}^J .

Cross-graph Feature Embedding in Graph Pairs Without interactive cross-graph feature aggregation, the direct node-to-node correspondence lacks

reliability [13]. Cross-graph feature embedding refers to the process of characterizing nodes and edges from different graphs, which is beneficial in improving the performance of graph matching [10]. To aggregate node features across graphs, we incorporate intra-graph affinity and cross-graph features using GCNs. Given two graphs \mathcal{G}^I and \mathcal{G}^J , the cross-graph feature embedding for node \mathbb{V}_i in \mathcal{G}^I is denoted in Eq. 3.

$$(v_i^I)^{(c)} = \psi_v^{(c)}([\sum_{j=1}^{n_J} \bar{S}_{ij}^{IJ} \cdot (v_j^J)^{(c)}, (v_i^I)^{(c)}]) \quad (3)$$

where $\psi_v^{(c)}$ is the MLP for c -th layer and $c \in \{1, \dots, C\}$. If $c = 1$, then $(v_i^I)^{(c)} = (v_i^I)^{(L)}$. We adopted the cross-graph feature embedding in Eq. 3 for C times to extract cross-graph hierarchical features and perform non-linear transformations. Symmetrically, for node \mathbb{V}_j in \mathcal{G}^J , the updated cross-graph feature embedding is calculated as $(v_j^J)^{(c)} = \psi_v^{(c)}([\sum_{i=1}^{n_I} \bar{S}_{ij}^{IJ} \cdot (v_i^I)^{(c)}, (v_j^J)^{(c)}])$. Finally, the affinity matrix is updated according to the updated cross-graph node feature embedding, as $\hat{S}_{ij}^{IJ} = \text{Sinkhorn}(\frac{(v_i^I)^{(C)} \cdot A \cdot (v_j^J)^{(C)}}{\sqrt{d}})$.

Multi-graph graph matching We first perform the feature embedding for each graph in \mathbb{G} according to Eq. 1. For each pair of graphs in \mathbb{G} , denoted as \mathcal{G}^I and \mathcal{G}^J , we calculate the joint node affinity matrix \hat{S}^{IJ} according to Eqs. 2 and 3 using cross-graph feature embedding. In MGM, we hypothesize that each graph contains the same number of nodes, i.e. $n_1 = n_2 = \dots = n_m = n$. Thus, $\hat{S}^{IJ} \in \mathbb{R}^{n \times n}$. For m graphs, the graph-matching results are denoted as a joint matching matrix $\hat{S} \in \mathbb{R}^{nm \times nm}$, as defined in Eq. 4.

$$\hat{S} = \begin{pmatrix} \hat{S}^{11} & \dots & \hat{S}^{1m} \\ \vdots & \ddots & \vdots \\ \hat{S}^{m1} & \dots & \hat{S}^{mm} \end{pmatrix} \quad (4)$$

where the diagonal-sub matrices \hat{S}^{II} are identical matrices and $I \in [1, \dots, m]$.

The goal of MGM is to maximize the matching score, as $S = \hat{y}^T \hat{S} \hat{y}$, where $\hat{y} \in \mathbb{R}^{nm}$ is a binary vector for the hard assignment of the graph matching for m graphs. Since \hat{S} is a symmetry matrix, according to Rayleigh's ratio theorem, the \hat{y} that will maximize S is the principal eigenvector of \hat{S} [15]. Thus, the MGM solution can be obtained by computing the maximum eigenvector of \hat{S} [14]. Mathematically, the eigenvector decomposition of \hat{S} is denoted in Eq. 5.

$$\hat{S} = U \Sigma U^T, \quad (5)$$

where $U = [\hat{U}^{1K}, \hat{U}^{2K}, \dots, \hat{U}^{mK}]^T \in \mathbb{R}^{nm \times n}$ is the n corresponding eigenvectors and $K \in [1, \dots, m]$; the diagonal matrix $\Sigma \in \mathbb{R}^{n \times n}$ contains top- n eigenvalues. Splitting the eigenvectors U to $\hat{U}^{iK} \in \mathbb{R}^{n \times n}$, we apply the MatchEIG algorithm [16] to generate the refined permutation matrix while considering the cycle

consistency during the MGM. The predicted hard-assignment matrix between graphs \mathcal{G}^I and \mathcal{G}^J is denoted in Eq. 6.

$$\hat{M}^{IJ} = \mathbf{Hungarian}((\hat{U}^{IJ}) \cdot (\hat{U}^{IJ})^T) \quad (6)$$

where the **Hungarian** algorithm [17] is commonly employed as a post-processing step to transform the doubly-stochastic matrix into the permutation matrix \hat{M}^{IJ} . To guarantee the cycle constancy, an arbitrary K is randomly selected[11].

2.3 Optimization and Testing

Optimization To train the proposed MGM, a set of graphs \mathbb{G} with m graphs is prepared. According to the annotated ICAs, the node correspondences between each arterial segment are obtained, resulting in the ground truth permutation matrix M^{IJ} for each pair of graphs \mathcal{G}^I and \mathcal{G}^J . If the arterial nodes $\mathbb{V}_i \in \mathcal{G}^I$ and $\mathbb{V}_j \in \mathcal{G}^J$ have identical labels, then $M_{ij}^{IJ} = 1$. To ensure consistency and accuracy, we select individual graphs exclusively from ICAs captured with the same view angle and the same number of arterial segments. The cross-entropy loss between the predicted permutation matrix \hat{M}^{IJ} and the ground truth M^{IJ} for each pair of graphs in the MGM setting is employed as the objective function, as defined in Eq. 7.

$$L = - \sum_{I=1}^m \sum_{J>I}^m \sum_{i=1}^n \sum_{j=1}^n (1 - M_{ij}^{IJ}) \log(1 - \hat{M}_{ij}^{IJ}) + (M_{ij}^{IJ}) \log(\hat{M}_{ij}^{IJ}) \quad (7)$$

Testing We first separate the entire dataset into three subsets, as D_{tr} , D_{te} and D_{tp} for the training set, the testing set and the template set with n_{tr} , n_{te} and n_{tp} ICAs, respectively. D_{tp} contains a set of representative ICAs selected by experienced cardiologists. We employ MGM to simulate the learning process, where cardiologists learn coronary artery anatomy by comparing a test case to multiple reference cases in D_{tp} . Given the intricate anatomy, clinical decisions hinge on multiple ICAs. During the testing, the tested ICA from D_{te} is denoted as \mathcal{G}^{te} and the other $m - 1$ ICAs are selected from D_{tp} and used to perform MGM; then a majority voting strategy is employed to assign semantic labels to matched arterial branches in D_{tp} . The testing algorithm is shown in Algorithm 1.

3 Experimental Results and Discussions

3.1 Implementation Details

All experiments were conducted with an NVIDIA RTX 4090 GPU on a Core I9-14900K. The number of GCN layers was set as $L = 2$ in Eq. 1 and the number of cross-graph feature embedding layers was set as $C = 2$ in Eq. 3. The dimension

Algorithm 1 The testing process of MGM for coronary artery semantic labeling. The **Combination** function indicates choosing $m - 1$ ICAs from n_{tp} ICAs in the template set.

Inputs: D_{te} with n_{te} ICAs; D_{tp} with n_{tp} template ICAs; m : number of MGM graphs

Outputs: labels for each segment of n_{te} ICAs in D_{te}

for $I = 1$ to n_{te}

1. for $J_1, J_2, \dots, J_{m-1} = \text{Combination}(n_{tp}, m - 1)$
 2. If $\mathcal{G}_{te}^I, \mathcal{G}_{tp}^{J_1}, \dots, \mathcal{G}_{tp}^{J_{m-1}}$ have same view angles and number of nodes
 3. Extract intra-graph features for $\mathcal{G}_{te}^I, \mathcal{G}_{tp}^{J_1}, \dots, \mathcal{G}_{tp}^{J_{m-1}}$
 4. Extract cross-graph features between each pair from $\mathcal{G}_{te}^I, \mathcal{G}_{tp}^{J_1}, \dots, \mathcal{G}_{tp}^{J_{m-1}}$
 5. Build joint matching matrix \hat{S} using Eqs. 3 and 4
 6. Perform eigenvector decomposition and graph matching using Eqs. 5 and 6
 7. Save $\hat{M}^{I, J_1}, \dots, \hat{M}^{I, J_{m-1}}$ for majority voting
 8. endif
 9. Assign labels to \mathcal{G}_{te}^I according to the majority voting among the set of \hat{M}^I .
 10. EndFor
-

of embedded features in Eq. 2 was set as $d = 256$. An Adam optimizer with an initial learning rate of $1e - 5$ was employed to train the model. 10% ($n_{tp} = 71$) of representative ICAs were selected as the template set and the remaining 90% ICAs were separated to D_{tr} and D_{te} to perform a five-fold cross-validation to evaluate the model performance. We evaluated the model performance using accuracy (ACC), macro precision (PREC), macro recall (REC) and macro F1-score (F1).

3.2 MGM for Coronary Artery Semantic Labeling

We first evaluate the proposed MGM for coronary artery semantic labeling. We set the number of graphs in \mathbb{G} as $m = \{3, 4\}$. The average performance of the five folds is reported in Table 2.

Table 2. Achieved performance for coronary artery semantic labeling using MGM

m	Artery	LMA	LAD	LCX	D	OM	macro Avg
3	ACC	99.62±0.47	96.18±0.94	93.96±2.44	94.59±1.26	90.96±3.57	94.71±1.75
3	PREC	99.62±0.47	96.05±0.96	94.09±2.43	94.44±1.29	91.15±3.54	95.06±1.63
3	REC	99.62±0.47	96.18±0.94	93.96±2.44	94.59±1.26	90.96±3.57	95.06±1.56
3	F1	99.62±0.47	96.12±0.94	94.02±2.44	94.49±1.27	91.05±3.56	95.06±1.02
4	ACC	99.60±0.49	94.21±1.33	92.92±1.92	91.52±2.16	89.41±3.00	93.04±1.22
4	PREC	99.60±0.49	94.21±1.21	92.93±1.98	91.51±1.96	89.42±3.10	93.53±1.18
4	REC	99.60±0.49	94.21±1.33	92.92±1.92	91.52±2.16	89.41±3.00	93.53±1.18
4	F1	99.60±0.49	94.21±1.27	92.92±1.95	91.51±2.06	89.41±3.05	93.53±1.19

According to Table 2, we observed that the proposed MGM achieved an impressive performance in coronary artery semantic labeling when the number of compared graphs was set to 3, with an ACC of 94.71%. However, when the number of compared graphs was set to 4, the performance slightly degraded, resulting in an ACC of 93.04%. This degradation may be caused by the limited number of graphs in our dataset, making it challenging to ensure cycle consistency, thus impacting the model’s performance. We also conducted experiments for $m = 5$ and $m = 6$; however, the performance was further deteriorated, with an ACC of 92.52% and 92.06%, respectively. Representative graph matching results are shown in Fig. 2.

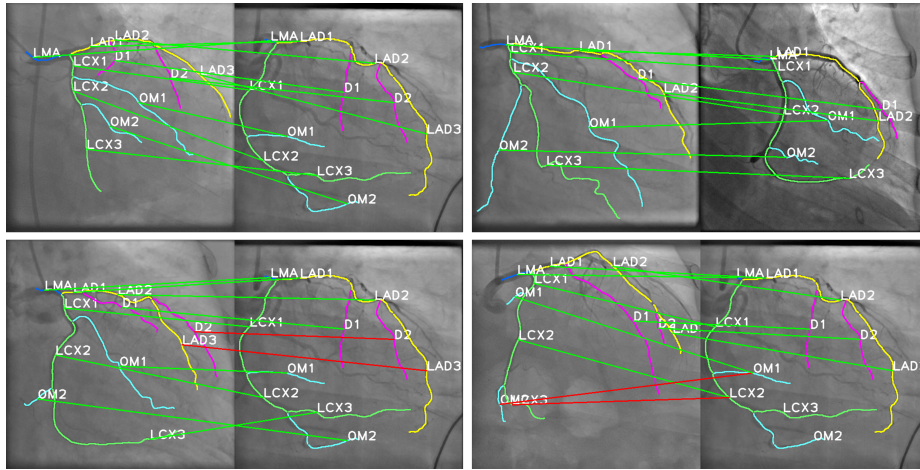


Fig. 2. Visualization of representative graph matching results. The green line indicates a correct match, while the red line represents an error.

3.3 Comparison with Competing Methods

We further compare our MGM approach with 4 deep learning-based methods for coronary artery semantic labeling, including (1) association graph-based graph matching network (AGMN) [4], which adopts the association graph for two-graph graph matching; (2) edge attention graph matching network (EAGMN) [5], which extends AGMN by adding the edge attention modules for feature embedding and two-graph graph matching; (3) neural graph matching (NGM), which employs the association graph-induced affinity matrix for two-graph graph matching; (4) bidirectional tree-LSTM (BiTL) [18], which employs tree-structured bidirectional LSTM for hierarchical feature extraction along with the vascular tree for coronary artery semantic labeling. For the graph matching-based methods, we adopted the same training strategy in MGM in splitting the datasets

into a training set, a testing set, and a template set. Also, the five-fold cross-validation was employed to evaluate the model. The comparison of the ACC among different methods is shown in Table 3.

Table 3. Achieved performance for coronary artery semantic labeling using MGM

Model	LMA	LAD	LCX	D	OM	macro Avg
BiTL	60.00±48.99	93.85±0.82	67.70±21.34	73.95±37.06	53.24±31.52	72.91±7.28
AGMN	99.07±0.31	87.30±4.40	86.46±2.74	83.20±3.91	80.80±4.11	86.39±1.82
EAGMN	99.42±0.64	89.31±2.95	88.43±3.93	85.18±3.73	79.68±4.31	87.67±1.88
NGM	98.85±1.22	92.23±3.41	89.67±3.24	90.07±4.66	84.08±4.80	90.39±3.54
Ours	99.62±0.47	96.18±0.94	93.96±2.44	94.59±1.26	90.96±3.57	94.71±1.75

Table 3 illustrates that our proposed MGM attained the highest macro ACC at 94.71% for coronary artery semantic labeling. While BiTL, designed for 3D CCTA datasets, proved unsuitable for ICAs, emphasizing the challenge of labeling coronary arteries from 2D images. Among graph matching-based methods, NGM, AGMN, and EAGMN concatenate node features and perform vertex embedding, while MGM conducts feature embedding and graph matching using the spectral method MatchEIG, preserving cycle consistency among multiple graphs. Results demonstrate that anatomical connections and cycle consistency between ICAs guide the matching process, ensuring matched arterial segments align not just in appearance or position but also in underlying anatomical structure. The success of MGM reinforces the significance of learning coronary anatomy across different ICAs in clinical practice, where cardiologists acquire knowledge by comparing a test case to multiple reference cases in a template set. MGM outperformed with the highest ACCs across all artery labeling types, highlighting the superiority of the usage of multi-graph graph matching for coronary artery semantic labeling.

4 Conclusion and Future Work

In this paper, we present a multi-graph graph matching-based method for coronary artery semantic labeling. Intra-graph and cross-graph GCNs were adopted to perform feature embedding, and a spectral-based method was employed to execute multi-graph matching assignments while considering cycle consistency. This method not only opens new avenues for improved analysis of vascular anatomy but also lays the foundation for multi-ICAs joint analysis. In the future, further exploration of coronary artery semantic understanding within ICA videos will be pursued.

References

1. Brown, J., Gerhart, T., Kwon, E. Risk factors for coronary artery disease, 2020

2. Li, Z., Zhang, Y., Liu, G., Shao, H., Li, W., Tang, X. A robust coronary artery identification and centerline extraction method in angiographies. *Biomedical Signal Processing and Control*, 16, pp.1-8. Elsevier (2015).
3. Zhao, C., Vij, A., Malhotra, S., Tang, J., Tang, H., Pienta, D., Xu, Z. and Zhou, W. Automatic extraction and stenosis evaluation of coronary arteries in invasive coronary angiograms. *Computers in biology and medicine*, 136, p.104667 (2021)
4. Zhao, C., Xu, Z., Jiang, J., Esposito, M., Pienta, D., Hung, G.U. and Zhou, W. AGMN: Association Graph-based Graph Matching Network for Coronary Artery Semantic Labeling on Invasive Coronary Angiograms. *Pattern Recognition*, vol. 143, pp. 109789 (2023)
5. Zhao, C., Xu, Z., Hung, G.U. and Zhou, W. EAGMN: Coronary artery semantic labeling using edge attention graph matching network. *Computers in Biology and Medicine*, vol. 166, pp. 107469 (2023)
6. Xian, Z., Wang, X., Yan, S., Yang, D., Chen, J. and Peng, C. Main coronary vessel segmentation using deep learning in smart medical. *Mathematical Problems in Engineering*, pp.1-9 (2020)
7. Parikh, N.I., Honeycutt, E.F., Roe, M.T., Neely, M., Rosenthal, E.J., Mittleman, M.A., Carrozza Jr, J.P. and Ho, K.K. Left and codominant coronary artery circulations are associated with higher in-hospital mortality among patients undergoing percutaneous coronary intervention for acute coronary syndromes: report From the National Cardiovascular Database Cath Percutaneous Coronary Intervention (Cath-PCI) Registry. *Circulation: Cardiovascular Quality and Outcomes*, 5(6), pp.775-782 (2012)
8. Khalil, E., Dai, H., Zhang, Y., Dilkina, B. and Song, L. Learning combinatorial optimization algorithms over graphs. *Advances in neural information processing systems*, vol. 30 (2017)
9. Vesselinova, N., Steinert, R., Perez-Ramirez, D.F. and Boman, M. Learning combinatorial optimization on graphs: A survey with applications to networking. *IEEE Access*, 8, pp.120388-120416 (2020)
10. Wang, R., Yan, J. and Yang, X. Combinatorial learning of robust deep graph matching: an embedding based approach. *IEEE Transactions on Pattern Analysis and Machine Intelligence*, vol. 45, p. 6984 - 7000 (2020)
11. Wang, R., Yan, J. and Yang, X. Neural graph matching network: Learning lawler's quadratic assignment problem with extension to hypergraph and multiple-graph matching. *IEEE Transactions on Pattern Analysis and Machine Intelligence*, vol. 44(9), pp.5261-5279 (2021)
12. Sinkhorn, R. A relationship between arbitrary positive matrices and doubly stochastic matrices. *The annals of mathematical statistics*, 35(2), pp.876-879. (1964)
13. Hou, Y., Hu, B., Zhao, W.X., Zhang, Z., Zhou, J. and Wen, J.R. Neural graph matching for pre-training graph neural networks. In *Proceedings of the 2022 SIAM International Conference on Data Mining*, pp. 172-180. Society for Industrial and Applied Mathematics. (2022)
14. Leordeanu, M. and Hebert, M. A spectral technique for correspondence problems using pairwise constraints. In *Tenth IEEE International Conference on Computer Vision*. vol. 2, pp. 1482-1489 (2005)
15. Johnson, C.R. and Horn, R.A. *Matrix analysis*. Cambridge: Cambridge University Press. (1985)
16. Maset, E., Arrigoni, F. and Fusiello, A. Practical and efficient multi-view matching. In *Proceedings of the IEEE International Conference on Computer Vision*, pp. 4568-4576 (2017)

17. Kuhn, H.W. The Hungarian method for the assignment problem. *Naval Research Logistics Quarterly*, vol. 2(1-2), pp.83-97.(1955)
18. Cao, Q., Broersen, A., de Graaf, M.A., Kitslaar, P.H., Yang, G., Scholte, A.J., Lelieveldt, B.P., Reiber, J.H. and Dijkstra, J. Automatic identification of coronary tree anatomy in coronary computed tomography angiography. *The International Journal of Cardiovascular Imaging*, 33, pp.1809-1819. (2017)
19. Avram, R., Olgin, J.E., Ahmed, Z., Verreault-Julien, L., Wan, A., Barrios, J., Abreau, S., Wan, D., Gonzalez, J.E., Tardif, J.C. and So, D.Y. CathAI: fully automated coronary angiography interpretation and stenosis estimation. *npj Digital Medicine*, vol. 6(1), p.142. (2023)
20. Zhang, H., Gao, Z., Zhang, D., Hau, W.K. and Zhang, H. Progressive perception learning for main coronary segmentation in X-ray angiography. *IEEE Transactions on Medical Imaging*, vol. 42(3), pp.864-879. (2022)
21. Akinlar, C. and Chome, E. PEL: a predictive edge linking algorithm. *Journal of Visual Communication and Image Representation*, vol. 36, pp.159-171. (2016)